Temperature response of ^{129}Xe depolarization transfer and its application for ultra-sensitive NMR detection

Leif Schröder[1,2],* Tyler Meldrum[1,2], Monica Smith[3,4], Thomas
J. Lowery[1,4,5], David E. Wemmer[1,4], and Alexander Pines[1,2]

[1]*Department of Chemistry, and* [3]*Biophysics Graduate Group; University of California, Berkeley*
[2]*Materials Sciences Division, and* [4]*Physical Biosciences Division;*
Lawrence Berkeley National Laboratory Berkeley, CA 94720 and
[5]*Current Address: T2 Biosystems, Cambridge, MA 02141*†
(Dated: May 23, 2008)

Trapping of exchangeable atomic xenon in functionalized cryptophane cages makes the high sensitivity of hyperpolarized (hp) ^{129}Xe available for highly specific NMR detection of biomolecules like proteins in solution. Here, we study the signal transfer onto a reservoir of unbound hp xenon by gating the residence time of the nuclei in the cage through the temperature-dependant exchange rate. Temperature changes were detectable immediately as an altered reservoir signal and nd makes it possible to detect temperature changes as small as ∼0.6 K. The temperature response is adjustable with lower concentrations of caged xenon providing more sensitivity at higher temperatures, allowing ultra-sensitive detection of such molecular cages at 310 K. Functionalized cryptophane was detected at concentrations as low as 10 nM, corresponding to a ∼4000-fold sensitivity enhancement compared to conventional detection. This sensitivity makes hp-NMR capable of detecting such constructs in concentrations far below the detection limit by benchtop UV-visible light absorbance.

PACS numbers: 82.56.-b

Nuclear magnetic resonance (NMR) is an extremely valuable detection tool in many fields of research because the recorded radio frequency (rf) signals are associated with almost no penetration limitations and extremely high specificity for the detected molecules. However, the method suffers from intrinsic low sensitivity. This can be overcome in some applications by use of hyperpolarized (hp) nuclei, but due to the nature of the hyperpolarization process it is difficult to make such high magnetization available for studies in biochemically relevant environments. Any detection scheme that enhances the sensitivity for biomolecular NMR applications is therefore of high interest.

Recent approaches for utilizing hp ^{129}Xe [1] in solution NMR exploit the fact that its resonance frequency is strongly shifted when it associates with a molecular cage such as cryptophane [2, 3]. Such cages can be functionalized with a targeting unit (antibody or ligand) to form xenon biosensors [4] in order to track a specific analyte upon biochemical binding. Biotinylated cage constructs are common examples for detecting avidin and protein-linked cages have the potential to bind to specific cell membrane receptors. Changes in the NMR signal of trapped ^{129}Xe occur upon interaction with the target and provide a powerful tool for spectroscopy and imaging. Hence, detection techniques that can identify caged Xe at low concentration ($< 10^{-6}$M) and are sensitive to the in situ physical environment will make NMR more competitive with optical and radioisotope detection.

A sensitive method of indirectly detecting exchangeable hp nuclei within cryptophanes has recently been reported (Hyper-CEST, [5]). Magnetization from encapsulated xenon can be "labeled" by a selective rf pulse that induces depolarization (i.e., saturation of the spin system). Depending on the exchange rate, hundreds to thousands of nuclei per second per cage experience this pulse, resulting in a depletion of the magnetization of free, dissolved xenon in the vicinity of the cage. This ensemble of uncaged xenon serves as a reservoir to detect the flow of saturated spins from the functionalized cage where the magnetization change is encoded.

Since chemical exchange rates are very sensitive to temperature T, the response of the Hyper-CEST effect upon changes in T is a promising tool to achieve high-sensitivity detection of the in situ environment and of the concentration of caged ^{129}Xe. Xenon atoms have been shown to reside in cryptophane cages in water for a few milliseconds at room temperature [2]. An increase in T significantly decreases this lifetime [6] and should amplify the Hyper-CEST effect. Here, we describe the direct response of the xenon reservoir signal intensity, $I_{\mathrm{res}}(t)$, in such a system to a temperature input function $T(t)$ in order to determine the sensitivity, dI_{res}/dT, of the ^{129}Xe NMR signal to temperature changes and to push the detection limit of functionalized cages into the nM concentration range.

A gas mixture of 89% He, 10% N_2 and 1% xenon (natural abundance of ^{129}Xe: 26%) was passed through a hyperpolarizer (XenoSpin$^{\mathrm{TM}}$, Amersham Health; Durham, NC) where spin exchange with optically pumped rubidium vapor [1] generates a ^{129}Xe nuclear spin polarization of ca. 5%. This mixture was delivered into an aqueous solution as described previously [7].

Figure 1 illustrates the ^{129}Xe NMR spectrum in D_2O

*Electronic address: LSchroeder@lbl.gov
†URL: http://waugh.cchem.berkeley.edu
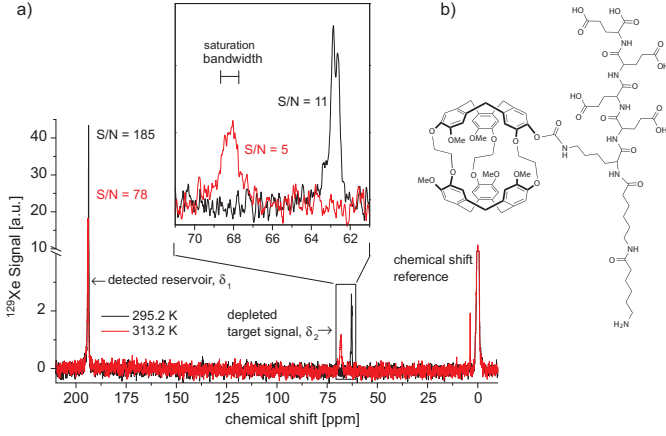
FIG. 1: (a) ^{129}Xe NMR spectrum illustrating that only a small fraction of xenon is associated with a functionalized cryptophane cage at $33\,\mu$M cage concentration. Increasing T from 295 K (black spectrum) to 313 K (red spectrum) shifts the signal of encapsulated xenon by ca. 5.5 ppm and induces accelerated chemical exchange that causes line broadening and decreases S/N. (b) Chemical structure of the functionalized cryptophane cage used in this study.

with a functionalized cryptophane-A cage designed as a universal precursor for biosensors that are prepared by attaching a targeting unit like biotin to the terminal amine group [9]. Data were recorded on an NMR spectrometer (Unity Inova; Varian Inc., Palo Alto, CA) at 7.05 Tesla with a 10 mm ^{129}Xe NMR probe. The resonance of the dissolved, uncaged xenon at $\delta_1 = 193.8$ ppm can be detected with a signal-to-noise ratio of S/N = 185 after 8 acquisitions at 295 K, whereas the diluted encapsulated xenon signal ($33\,\mu$M cage concentration) at $\delta_2 = 62.7$ ppm gives only a S/N = 11.

For this experiment, Hyper-CEST detection used a frequency-selective saturation pulse of 500 ms (amplitude $B_1 = 6.48\,\mu$T, bandwidth $\Omega = 0.93$ ppm) centered at δ_2, followed by observation of the subsequent change in the reservoir signal. Previous studies showed that the resonance frequency of the caged xenon shifts linearly with temperature [6]. This effect requires that the saturation carrier frequency ω_{sat} be swept to ensure optimum activation of the Hyper-CEST effect when studies extend over substantial temperature ranges and use narrow bandwidth saturation pulses. Comparing spectra at 295 K and 313 K showed a shift of 26.6 Hz/K for the resonance of caged xenon (Tab. I) for this molecule. In contrast, the reservoir signal shift of 3 Hz/K is insignificant and should not require parameter adjustments for this system.

The substantial exchange line broadening associated with increasing temperature causes a linewidth for trapped ^{129}Xe of ca. 74 Hz at 313 K compared to ca. 40 Hz at 295 K. Hence, thermometric resolution based on direct observation of encapsulated Xe is reduced from $\sim$0.15 K to 0.28 K at 313 K [10]. While direct observa-

TABLE I: Frequency offsets of the line positions of the reservoir signal (ω_1) and caged xenon (ω_2) relative to the ^{129}Xe standard frequency of the spectrometer.

T [K]	ω_1 [Hz]	ω_2 [Hz]
295	14,972.0	4,110.7
313	15,025.5	4,590.0
$\Delta T = 18$ K	shift = 3.0 Hz/K	shift = 26.6 Hz/K

tion of caged xenon requires relatively high concentrations of the construct (or extensive signal averaging), thermometry via saturation transfer into the reservoir works at much lower concentrations. However, sweeping ω_{sat} to scan for maximum saturation revealing $\delta_2(T)$ is time consuming and becomes less accurate with increasing T due to the above-mentioned line broadening. Detecting $I_{\mathrm{res}}(T)$ instead of $\delta_2(T)$ yields higher sensitivity to temperature changes and is achieved in only two acquisitions.

For illustrating this approach, the temperature of the biosensor sample was varied over time, serving as a characteristic input function $T(t)$, and the change in $I_{\mathrm{res}}(t)$ was observed. To compensate for line shape changes at high temperatures, $I_{\mathrm{res}}(t)$ was determined by integrating over a bandwidth of 70 Hz centered at δ_1 to guarantee reproducible observation of the Hyper-CEST response. Starting at $T = 287$ K and $\omega_{\mathrm{sat}} = 3906.7$ Hz, the sample was heated up to $T = 313$ K in steps of 2 K using the variable temperature unit of the spectrometer. To allow for stabilization of T within the solution, an acquisition was started every 7 minutes. Cooling of the sample to 287 K was performed at twice the rate that it had been heated, followed by an adjustment to room temperature (Fig. 2a).

Figure 2b shows the response of $I_{\mathrm{res}}(t)$ to $T(t)$ which is clearly the inverse of the saw-tooth input function, corresponding to increased depolarization transfer upon increasing temperatures and vice versa. To calibrate the temperature sensitivity of this sensor, data from Fig. 2b was used to plot I_{res} vs. T as shown in Fig. 3a. Signal intensity from an acquisition without a saturation pulse (see dashed line in Fig. 2b) was used to normalize all data points. The temperature dependence can be modeled with an empirical fit to a sigmoidal Boltzmann function (correlation coefficient $R^2 = 0.98$)

$$I_{\mathrm{res}} = A_1 + \frac{A_2 - A_1}{1 + e^{(T-T_0)/dT}} \qquad (1)$$

with $A_1 = 0.04 \pm 0.04$, $A_2 = 1.00 \pm 0.05$, $T_0 = (297.5 \pm 0.5)$ K, and $dT = (3.9 \pm 0.6)$ K^{-1}. The derivative of this function yields the differential temperature sensitivity dI_{res}/dT plotted in Fig. 3b (solid line), showing a maximum sensitivity of ca. 6% decrease per K around 297.5 K. Since the systematic noise is about 3.6% (see below), this corresponds to temperature resolution of ca. 0.6 K.

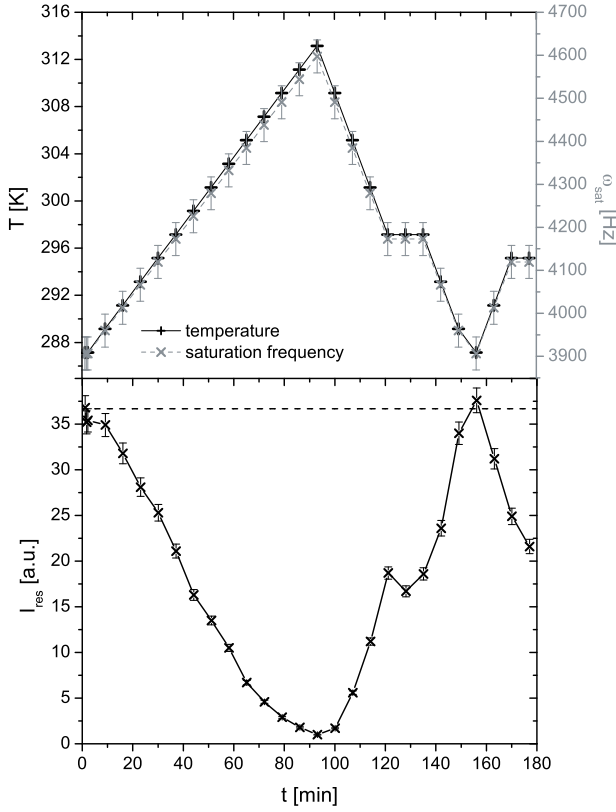The differential sensitivity is adjustable to some ex-

FIG. 2: (a) Input function $T(t)$ (black solid line) for Hyper-CEST signal transfer using the construct shown in Fig. 1. The saturation frequency offset ω_{sat} (grey dashed line) is adjusted according to the resonance shift of 26.6 Hz/K. Bars indicate the bandwidth of the saturation pulse of $\Omega = 76.7$ Hz (0.925 ppm). (b) Response $I_{res}(t)$ to $T(t)$. Varying the temperature changes ^{129}Xe signal transfer through the cage that is present at $27.2\,\mu$M. The reference signal for no saturation transfer is illustrated by the dashed line.

FIG. 3: (a) Calibration for temperature sensitivity of I_{res} shown in Fig. 2b at $27.2\,\mu$M cage concentration ($\times$) and for $11.2\,\mu$M cage concentration ($+$). The signal intensity is normalized to a control experiment without saturation pulse. Data are fitted to Eq. 1. and shown with a 95% confidence band (dashed lines). (b) The differential sensitivity of ^{129}Xe signal, intensity change per Kelvin, is given by the first derivative of the fit results in a). Reducing the concentration of the cage construct shifts the maximum sensitivity to higher temperatures. Since the experimental standard deviation in determinating of I_{res} is $\sim$3.6% (see below), the temperature resolution is limited to ca. 0.6 K for the $27.2\,\mu$M solution.

tent by adjusting certain system parameters. For example, lower cage concentrations, shorter saturation pulses, or lower saturation power would all yield less efficient saturation transfer at a given T, thus shifting the Boltzmann function to the right. This was demonstrated with a solution of $11.2\,\mu$M cage concentration (only one temperature sweep from 293 K to 313 K in this case). As seen in Fig. 3a, the overall saturation is decreased and the Boltzmann transition stretched over a wider temperature range ($A_1 = 0.11 \pm 0.03$, $A_2 = 1.00 \pm 0.03$, $T_0 = (303.7 \pm 0.3)$ K, $dT = (5.7 \pm 0.5)$ K^{-1}, $R^2 = 0.99$). In addition, the range of maximum sensitivity is shifted by 6.2 K to give a high-T sensitivity (Fig. 3b, dashed line). Similarly, a low-T sensitivity can be achieved by opposite modifications.

The significant increase in saturation transfer upon increasing T shown in Fig. 3a can be used to detect very low concentrations of caged xenon. To determine the detection threshold for this construct at body temperature (ca. 310 K), a solution of 10 nM concentration was
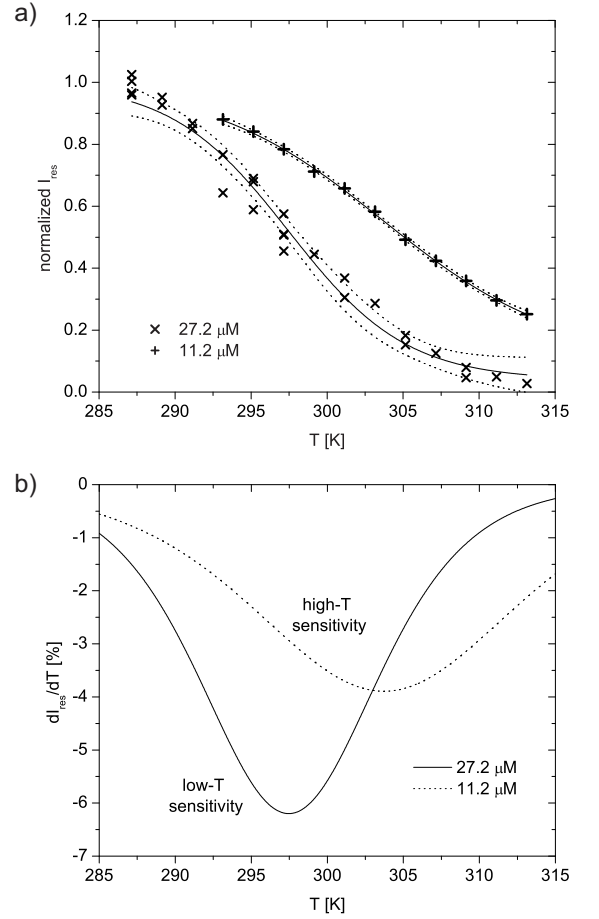
prepared. Figure 4 illustrates that Hyper-CEST induces a signal decrease of $\sim$16% with this concentration after 20 s saturation with a pulse amplitude of $B_1 = 25.8\,\mu$T ($\Omega = 544$ Hz). The standard deviation (SD) of the signals detected in control experiments with off-resonance saturation was 3.6%.

To estimate the sensitivity gain compared to direct detection shown in Fig. 1, parameters summarized in Tab. II were used. The xenon occupancy of the cages calculated from the binding constant, $K = 6000$ M^{-1} [7], is 53% [11]. This information must be considered when designing cages with different affinity for the noble gas [3]. The saturation transfer observed in Fig. 4 is caused by a concentration of caged ^{129}Xe that is only 1.4 nM.

TABLE II: Experimental parameters for comparison of direct and indirect detection. The amount of detectable, encapsulated xenon, i.e. $[^{129}\text{Xe}]_{\text{cage}}$, is determined by the concentration of the cryptophane cage, the abundance of the isotope ^{129}Xe (26%) and the xenon partial pressure of the gas above the solution. The final acquisition time is determined by the # of scans and the repetition time TR.

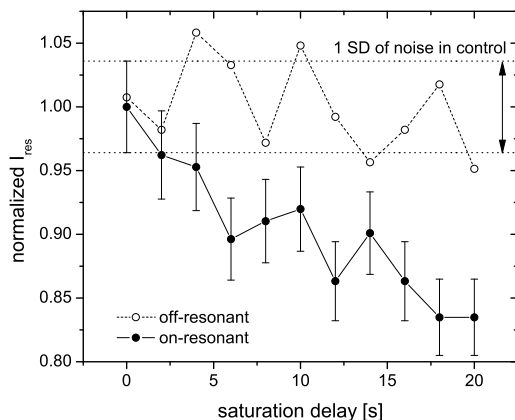|	[cage] [nM]	max. $[^{129}\text{Xe}]_{\text{cage}}$ [nM]	$[^{129}\text{Xe}]_{\text{cage}}$ @ 58.4 mbar [nM]	# scans	TR [s]	S/N	T [K]
direct detection	33,500	8,710	4,616	8	33	5.1	313.2
Hyper-CEST detection	10	2.6	1.38	2	53	4.6	310.2

FIG. 4: High-sensitivity detection of 1.4 nM encapsulated xenon signal (10 nM cage present) in D_2O at 310 K. The SD in the control dataset is 3.6% and is systematic noise due to imperfections in the xenon delivery. Maximum signal depletion is 16% of a resonance that was detected with a S/N of 110. However, the limiting factor for the Hyper-CEST detection is the variability of 3.6% in the off resonance experiment, so S/N for indirect sensor detection is 16.5/3.6 = 4.6.

Even though the S/N of direct detection at 310 K will be slightly higher than at 313 K (ca. 6 instead of 5.1[12]), this comparison still yields a ∼4000-fold sensitivity enhancement with respect to direct detection; the direct measurement time would be ∼55 years to achieve the same S/N rather than 106 seconds.

Under conditions described here the exchangeable, hyperpolarized xenon detection makes NMR much more sensitive than optical methods in this specific case. Conventional, benchtop UV-visible absorbance detection of the cryptophane-A cage ($\epsilon_{282} = 8000\,\text{M}^{-1}\text{cm}^{-1}$, [8]) requires a minimum concentration of $\sim 1\,\mu\text{M}$ [13]. Thus the temperature-controlled depolarization transfer detection is very promising for new applications of high-sensitivity NMR with functionalized biosensors.

[1] B. M. Goodson, Concepts Magn. Res. **11(4)**, 203 (1999).
[2] K. Bartik, M. Luhmer, J.-P. Dutasta, A. Collet, and J. Reisse, J. Am. Chem. Soc. **120**, 784 (1998).
[3] G. Huber et al., J. Am. Chem. Soc. **128**, 6239 (2006).
[4] M. M. Spence et al., Proc. Natl. Acad. Sci. USA **98**, 10654 (2001).
[5] L. Schroder, T. J. Lowery, C. Hilty, D. E. Wemmer, and A. Pines, Science **314**, 446 (2006).
[6] T. J. Lowery et. al., ChemBioChem **7**, 65 (2006).
[7] S.-I. Han et al., Anal. Chem. **77(13)**, 4008 (2005).
[8] M. M. Spence, E. J. Ruiz, S. M. Rubin, T. J. Lowery, N. Winssinger, P. G. Schultz, D. E. Wemmer, and A. Pines, J. Am. Chem. Soc. **126**, 15287 (2004).
[9] In contrast to previously used constructs, this one has a negatively charged side chain to minimize interactions with the glass wall and remain detectable at low concentrations

[10] For sufficient S/N, resonance shifts of ca. 10% of the line width can be detected, thus 4 Hz is the resolution limit at 295 K, yielding ca. 0.15 K thermal resolution.
[11] Xenon dissolves in water to a concentration of $190\,\mu\text{M}$ at 310 K and 58.4 mbar partial pressure, which, together with $K = 6000\,\text{M}^{-1}$, yields an occupancy of 53%.
[12] Based on data in [6], the exchange rate increases by a factor of ~ 14 for $T = 22°\text{C} \rightarrow 40°\text{C}$ but only by ∼9 for $T = 22°\text{C} \rightarrow 37°\text{C}$; the corresponding line broadening would then reduce S/N from 11 to 6
[13] Extinction coefficients can be as high as $100{,}000\,\text{M}^{-1}\text{cm}^{-1}$ for many macromolecules, thus being ca. 12 times more sensitive than for cryptophane. However, this would still yield a minimum concentration of ca. 400 nM for detection with UV-vis absorbance.